Membrane and Water Treatment, *Vol. 17, No. 4 (2026) 311-321*
https://doi.org/10.12989/mwt.2026.17.4.311

Techno-Press

Holey graphene oxide/methylene blue composite membrane with high flux for water treatment

Xuan Liu[1a], Shihao Li[1], Hangdong Chen[1], Xiang Yu[1], Mingyang Li[1], Yafei Zhang*[2], Bin Li[3b], Nantao Hu[2]

[1]*College of Engineering, Shanghai Ocean University, 999 Huchenghuan Road, Pudong New Area District Shanghai, P.R.China*
[2]*Key Laboratory for Thin Film and Microfabrication Technology of the Ministry of Education, School of Electronics, Information and Electrical Engineering, Shanghai Jiao Tong University, No. 800, Dongchuan Road, Minhang District, Shanghai, P.R.China*
[3]*Research Center for Photovoltaics, Shanghai Institute of Space Power-Sources, Shanghai, 200245, China*

(Received July 6, 2023, Revised April 9, 2026, Accepted June 23, 2026)

Abstract. Two key factors limiting the industrial application of graphene oxide membranes are low water flux and easy swelling in water during operation. In this study, a novel holey graphene oxide/methylene blue (HGO/MB) composite membrane was prepared by vacuum filtration using a two-step method, including chemical etching graphene oxide (GO) with H_2O_2 to improve the water flux and then intercalating MB into HGO to limit the swelling of GO membranes effectively. The composite membrane showed a higher pure water flux of 23.4 L/m^2·h·bar, which was improved about 6 times compared to GO membrane. The rejection rates of the membrane for Na_2SO_4, methyl orange (MO) and rhodamine B (Rh B) reached 83.2%, 93% and 97%, respectively. HGO/MB composite membrane remained stability after 15 min of ultrasound treated because of the π - π conjugation and electrostatic interaction between HGO and MB. This study demonstrated that the membranes prepared have effectively improved water flux and stability without loss of rejection, which held great potential for water treatment applications.

Keywords: holey graphene oxide; membrane; methylene blue; water treatment; π - π conjugation

1. Introduction

Water pollution has been a serious problem with the exponential rise in population and industrialization [1-6]. Membrane separation technology can solve this problem effectively due to its advantages including energy saving, perfect selectivity, convenient operation, negligible chemical reaction, and small impact on the environment 2016) [7-9]. In recent years, a variety of two-dimensional nanomaterials such as molybdenum disulphide (MoS_2) [10], silica (SiO_2) [11], metal-organic frameworks (MOFs) [12, 13], Carbon nanotubes (CNTs) [14], and MXene [15, 16] have been used in the research and development of membrane separation technology with good results. As a typical two-dimensional nanomaterial, GO [17, 19] has raised a lot of attention from

*Corresponding author, Professor, E-mail: yfzhang@sjtu.edu.cn
[a]Ph.D., E-mail: xliu@shou.edu.cn
[b]Ph.D., E-mail: tolb10@163.com

ISSN: 2005-8624 (Print), 2092-7037 (Online)

researchers.

GO has a very great potential for the preparation of nanofiltration membranes with excellent chemical stability, robust mechanical properties and large specific surface area [20-22]. Moreover, GO is rich in oxygen-containing functional groups, such as epoxy groups(-O-), carboxyl(-COOH), carbonyl(C=O), and hydroxyl(-OH), which endow the surface of GO hydrophilicity and electronegativity as well as benefit modification of GO [23-25]. Nevertheless, the inherent instability of GO membranes greatly hinders the practical use of GO membranes, which is caused by various factors such as weak binding, hydration effect, and disordered accumulation of GO nanosheets [26, 27].

Reduction or chemical cross-linking of GO can effectively enhance its stability in water [28], but these methods have practical limitations, such as being time-consuming, non-scalable, difficult to replicate, or all of the above [29, 10]. Recently, the intercalation by π-π conjugation and electrostatic interaction has gained widespread attention for its simplicity and effectiveness [29, 30]. The GO-NG composite membrane (GNM) was prepared by intercalating N-doped graphene (NG) into GO membranes (GOMs), which possesses an improved stability and a three times water flux compared to unmodified graphene [31]. Using MB as a modifier, GO/MB composite membrane was fabricated and remained stable for 55 h of continuous testing, but the water flux need to be ameliorated urgently [29].

The high tortuosity of water flow through GO membranes is a significant contributor to their low water flux. However, the introduction of in-plane nanopores on the GO nanosheets is a viable and uncomplicated solution to alleviate this problem [32, 33]. HGO membranes were prepared by holey GO, which increases the water flux by about four times compared to conventional GO membranes while increasing the thickness [34]. As to other rHGO membranes fabricated by reduced holey GO, the water flux increased significantly compared to that of rGO membranes [35]. Therefore, in-plane nanopore generation on GO nanosheets is an effective method to improve water flux.

Here, novel HGO/MB composite membranes were prepared by a two-step method, including chemical etching of GO with H_2O_2 to improve the water flux and then intercalating MB into HGO to limit the swelling of GO membranes effectively. The results demonstrated that the HGO/MB composite membranes prepared exhibited excellent water permeability, good rejection and high stability and possessed potential application in water treatment.

2. Experimental

2.1 Materials

Graphite powder was purchased from Shandong Jinlilai Co. (China). H_2O_2 (30 mass % in H_2O), Na_2SO_4(≥99.0%), methylene blue(MB), rhodamine B(Rh B), methyl orange(MO), etc. were purchased from Sinopharm Chemical Reagent Co. (China). All the materials and reagents were used in their original form without any additional purification steps.

2.2 Methods

2.2.1 Preparation of HGO

GO was prepared from graphite with a modified Hummers' method [32, 36]. HGO was prepared by adding 5ml of 30% H_2O_2 to 50mL 2mg/mL GO aqueous solution and then heated at

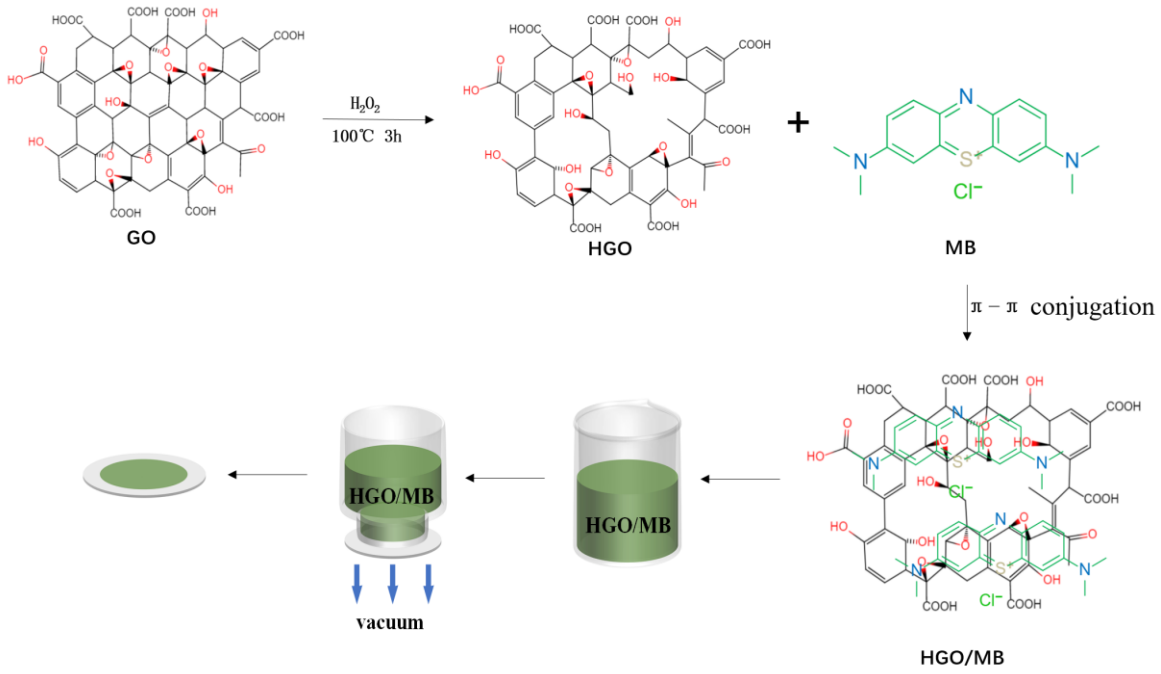

Figure 1. Schematic illustration of the fabrication process of HGO/MB membrane

100℃ for 3h under stirring. The reacted solution was cooled to room temperature and then purified by dialysis to remove the residual H_2O_2. Finally, deionized water was added to form a 1mg/ml HGO water dispersion.

2.2.2 Preparation of HGO/MB composite membranes

100 mL of deionized water was added into 0.5 mL 1mg/ml HGO water dispersion, followed by stirred well and ultra-sonicated for 5 min, which was marked as solution A. 0.05 g/L MB water dispersion was prepared by dissolving 5 mg of MB into 100 mL of deionized water. Different volumes (0 μL ,100 μL, 200 μL, 300 μL) of MB water dispersion were added into 100 ml of deionized water and stirred vigorously for 1 min, and the obtained solutions were marked as solution B0, B1, B2, B3 respectively. Solution B0-B3 was added to solution A with vigorous stirring for more than 3 h to obtain the HGO/MB water dispersion. The water dispersion was then vacuum filtered onto a microporous polyethersulfone(PES) membrane to prepare the HGO/MB composite membrane. The HGO/MB membranes were called HGO, HGO/MB-100, HGO/MB-200, and HGO/MB-300 based on the volume of the added MB water dispersion. GO membranes were fabricated by vacuum filtration method for companion with HGO/MB membranes. The fabrication process of HGO/MB membrane was shown in Fig. 1.

2.3 Characterizations

Pore size of HGO was analyzed by surface area and porosity analyzer (ASAP 2460, Micromeritics Instrument (Shanghai Ltd.). Morphology of membranes were characterized by

scanning electron microscopy (SEM, Gemini SEM7426, ZEISS, Germany). Membranes structure was analyzed by Raman spectrometer (inVia, RENISHAW). UV-Vis absorption spectrometer (UV-VIS, LAMBDA950, PerkinElmer) was used to analyze interactions and detect the dye concentration. The interlayer spacing of the membranes underwent X-ray diffraction testing (XRD, D8 ADVANCE, BRUKER, Germany). A water contact angle (WCA, DSA30, KRUSSA, Germany) measurement was carried out to assess the hydrophilicity of the membranes. The salt concentrations were tested by sodium ion concentration meter (DWA-51, Hangzhou Qiwei Instrument Co., Ltd.).

2.4 Membrane performance test

2.4.1 Permeance and rejection properties of the membranes

During the experiment, the water flux and rejection rate of the membranes were assessed using a cross-flow device, with a membrane effective area of approximately 3.14 cm^2. Dyes (Rh B and MO, at a concentration of 50 mg/L) and salt solution (Na_2SO_4, at a concentration of 1000 ppm) were employed to test rejection performance at 1 bar. The permeation J ($L/m^2 \cdot h \cdot bar$) and rejection R (%) were calculated according to Eq. (1, 2) respectively:

$$J = \frac{V}{A\Delta tP} \tag{1}$$

$$R = \left(1 - \frac{C_p}{C_f}\right) \times 100\% \tag{2}$$

where V (L) is the volume of permeate water, A (m^2) is the effective membrane area, Δt(h) is the filtration time, and P (bar) is the pressure imposed on membrane surface. Cp and Cf are the concentration of permeate and feed solution, respectively.

3. Results and discussion

3.1 Membrane characterization

A surface area and porosity analyzer was employed to measure the specific surface area and pore size distribution of GO and HGO samples. N_2 adsorption/desorption isotherms of all samples were shown in Fig. 2(a). It is found that the specific surface area of HGO (37.005 m^2/g) was higher than that of GO (28.348 m^2/g), which was ascribed to the existence of more nanopores in the basal plane of HGO nanosheets [38, 39]. The pore size distributions of HGO and GO were show in Fig. 2(b). HGO exhibited more mesopores than GO and the pore size of HGO was concentrated in 1-3 nm. The results indicate that using H_2O_2 oxidation is a useful approach for creating nanopores on GO nanosheets, which can effectively reduce the tortuosity of water channels (Fig. 3) and improve the water flux.

The SEM was employed to analyze the surface morphology of the membranes, which is illustrated in Fig. 2(c, e). The increase of wrinkles on the surface of HGO membrane after treatment with H2O2 was due to a large number of defects formed in GO during the reaction process [33, 24]. After addition of MB, some defects of HGO were repaired, and HGO nanosheets became more compact due to the π-π conjugation and electrostatic interaction between HGO and MB, so the wrinkles were reduced [31, 40].

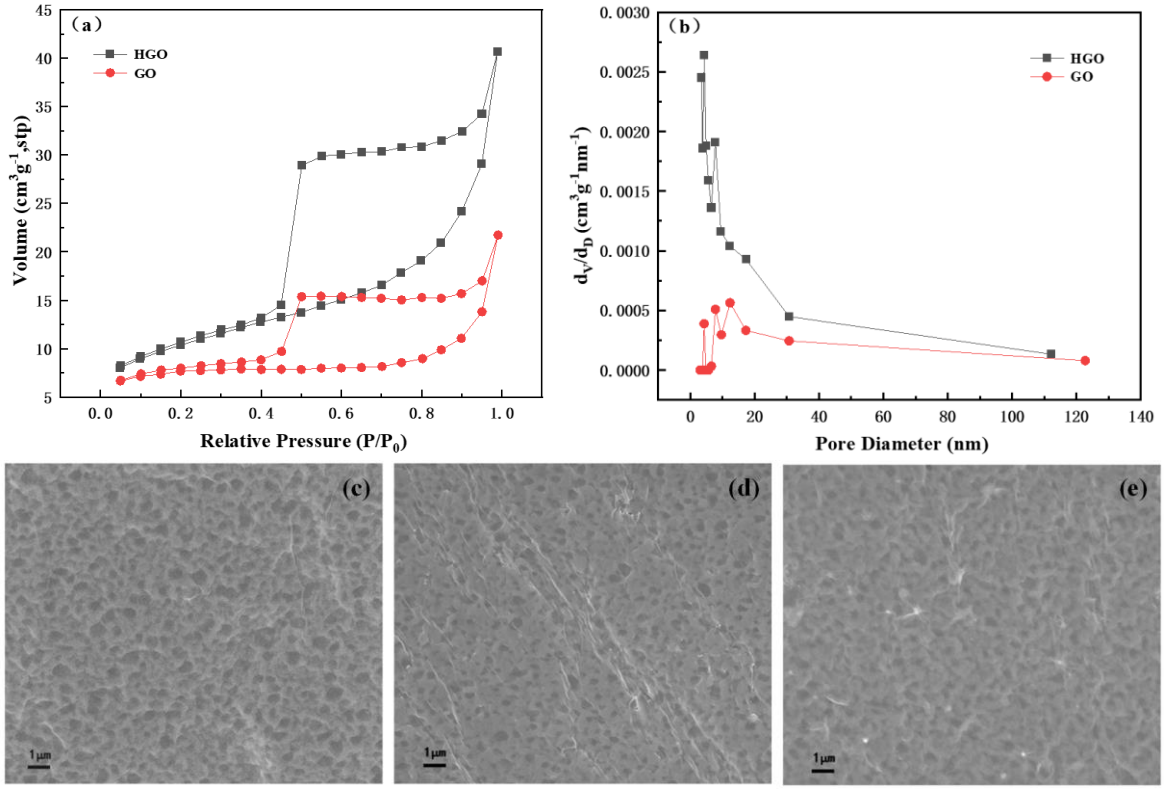

Figure 2. (a) Nitrogen adsorption/desorption isotherms and (b) pore size distributions of HGO and GO. SEM images of (c)GO membrane, (d)HGO membrane and (e) HGO / MB membrane

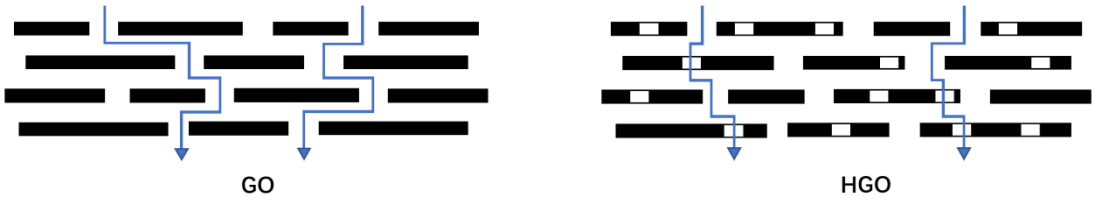

Figure 3. Water transport routes in GO and HGO membranes

The microstructure of GO, HGO and HGO/MB membranes was further analyzed by Raman spectra and showed in Fig. 4(a). It can be seen that there were two characteristic peaks, corresponding to the D band and G band, respectively [41]. The D band is linked to the structural defects and disordered arrangements of GO, whereas the G band is associated with in-plane vibrations of sp2 hybridized carbon domains [32,35,37]. The degree of disorder and defects (such as wrinkles, folds, pores, and edges) present on the GO nanosheet can be determined by evaluating the intensity ratio of the D band to the G band (ID/IG) [24]. It was noteworthy ID/IG value of GO was 0.76, while ID/IG value of HGO increased to 0.80 owing to the increase of defects in the membrane by chemical etching. After MB was intercalated into HGO, ID/IG value decreased to 0.78 due to the reduced wrinkles. This was consistent with SEM analysis results.

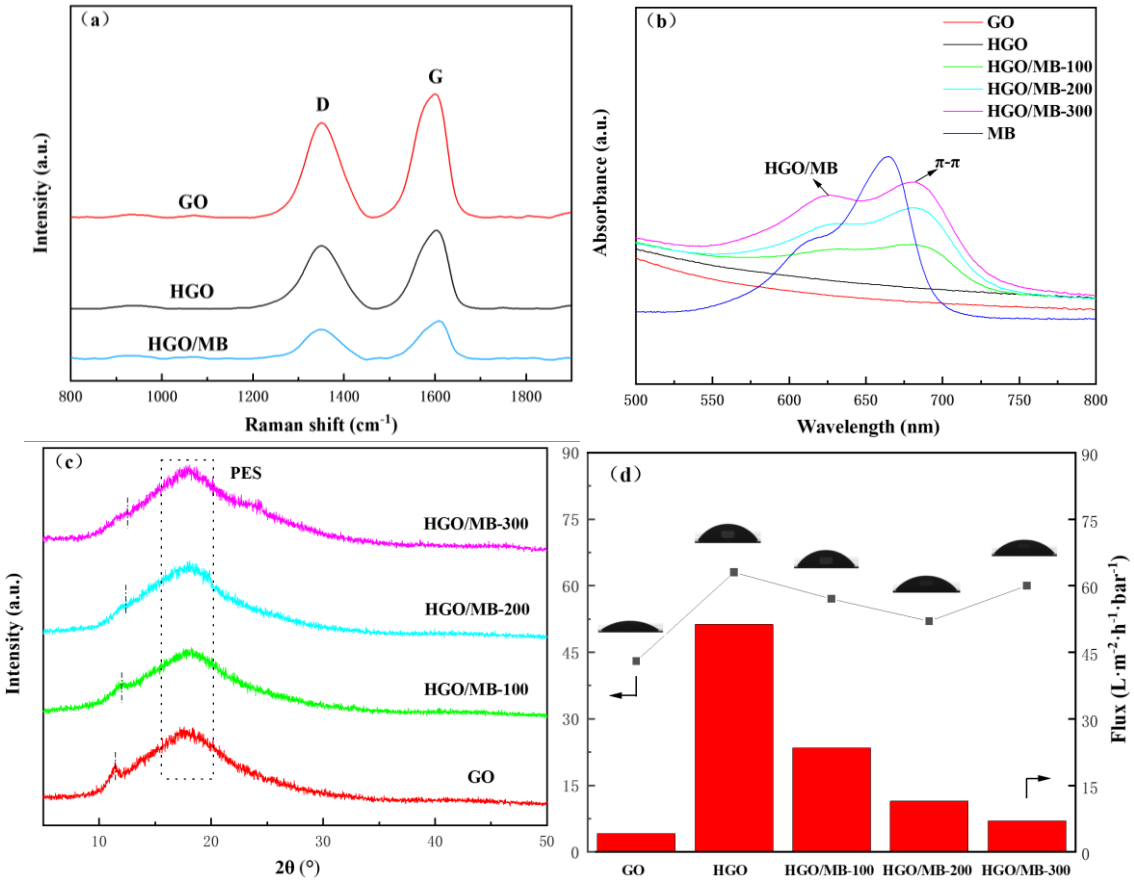

Figure 4. (a) Raman spectra of GO, HGO and HGO / MB membrane; (b) UV spectra of GO, HGO, HGO / MB dispersion and MB; (c) XRD pattern of GO and HGO / MB membrane; (d) Water contact angle and pure water flux of GO, HGO and HGO / MB membrane

UV spectra of GO, HGO, HGO / MB dispersion and MB were shown in Fig. 4(b). The MB spectra showed the presence of two peaks at 608 nm and 662 nm, which subsequently underwent a shift to 620 nm and 670 nm, respectively, upon mixing with HGO. The phenomenon was due to HGO/MB monolayer adsorption and π-π conjugation between HGO and MB, respectively [42,43]. When the amount of MB was gradually increased, the peaks at 620 nm and 670 nm became more and more obvious, showing that monolayer adsorption was increasing and π-π conjugation was also enhancing, which was beneficial for enhancing membrane stability.

XRD was employed to investigate the d-spacing of the membranes, as shown in Fig. 4(c). The membrane samples underwent a drying process before they were tested. GO membrane had a typical peak of around 11° [29], which gradually and inconspicuously shifted to the right with increasing MB content. When the volume of MB dispersion reached 300μL, the diffraction peak moved to about 12°, which indicated that the introduction of MB reduced the d-spacing of the membrane owing to π-π conjugation and electrostatic interactions between HGO and MB [29, 4].

As shown in Fig. 4(d), to assess the hydrophilicity of the membranes, the WCA was measured. The WCA of GO was 43°, while the WCA of HGO increased to 63° because of the reduced

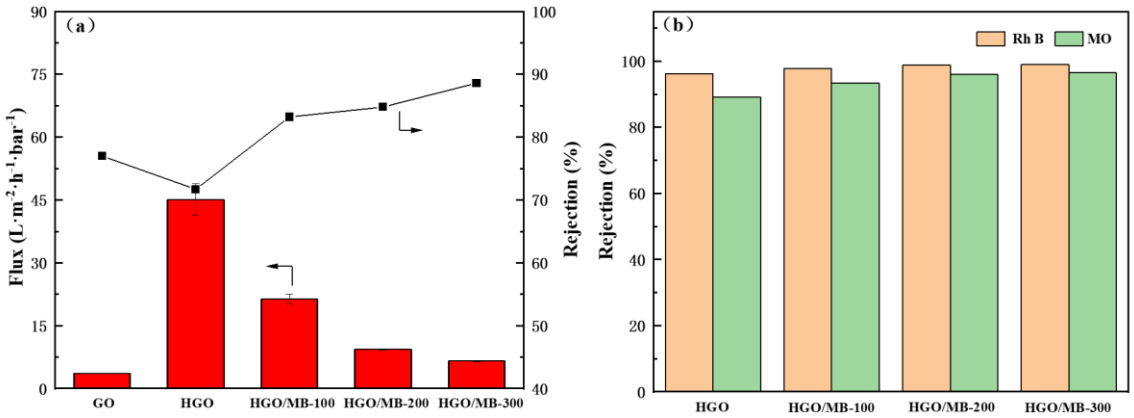

Figure. 5 (a) The water flux and rejection rate of Na2SO4; (b) Rejection rates of Rh B and MO

oxygen-containing functional groups of HGO after chemical etching [44, 39]. When a small volume of MB (<=200uL) was added to HGO dispersion, the WCA of HGO/MB-200 decreased to 53° since the heterocyclic structure and charged groups of MB endowed MB with excellent water solubility [29]. However, when the volume of MB increased to 300 μL, WCA of HGO/MB-300 increased to 60°, which was caused by two reasons. First, the π-π conjugation and electrostatic interactions affected the benzene rings on either side of the heterocyclic structure, leading to a loss of freedom in the heterocyclic structure [29, 42]. Second, the carboxyl group on GO selectively interacted with MB through electrostatic interactions [29].

3.2 Membrane performance test

Fig. 5(a) showed the water flux and rejection rates of the GO, HGO and HGO/MB membranes in Na_2SO_4 salt solution tested by a cross-flow device. The water flux of HGO membrane was 45.12 L-m^{-2}-h^{-1}-bar^{-1}, which was about 15 times of GO membrane. This was because that the large number of in-plane nanopores on the HGO nanosheets reduced tortuosity and thus increased water permeance [32]. The water flux of HGO/MB membrane gradually decreased and the Na_2SO_4 rejection rate gradually increased as the increasing MB addition, which was due to the decrease of d-spacing of the membrane under the π-π conjugation and electrostatic effect and the repair of some defects of HGO [29, 40, 30]. In addition, MB in the interlayer impeded the passage of water molecules, which was also the reason for the decreased water flux [29]. At a MB volume of 100 μL, the Na_2SO_4 rejection rate was 83.2%, and the water flux was about 7 times higher than that of the GO membrane, measuring at 21.34 L/m^2·h·bar. HGO/MB composite membrane showed a higher pure water flux of 23.4 L/m^2·h·bar (Fig.4(d)), which was improved about 6 times compared to GO membrane. Fig. 5(b) showed the rejection rates of Rh B and MO dyes by HGO and HGO/MB membranes. The rejection rate of HGO/MB membrane for both dyes was above 93%, with the highest rejection rate of 95.9% for MO and 98.9% for Rh B.

The stability of GO, HGO and HGO/MB membrane was observed by ultrasonic experiments as shown in Fig. 6. The GO and HGO membrane started to decompose at 5min of ultrasound and detached obviously after 15min. In contrast, HGO/MB membrane was almost unchanged in 0-15 min, which was mainly attributed to the π-π conjugation and electrostatic interactions that improved the stability of the membrane.

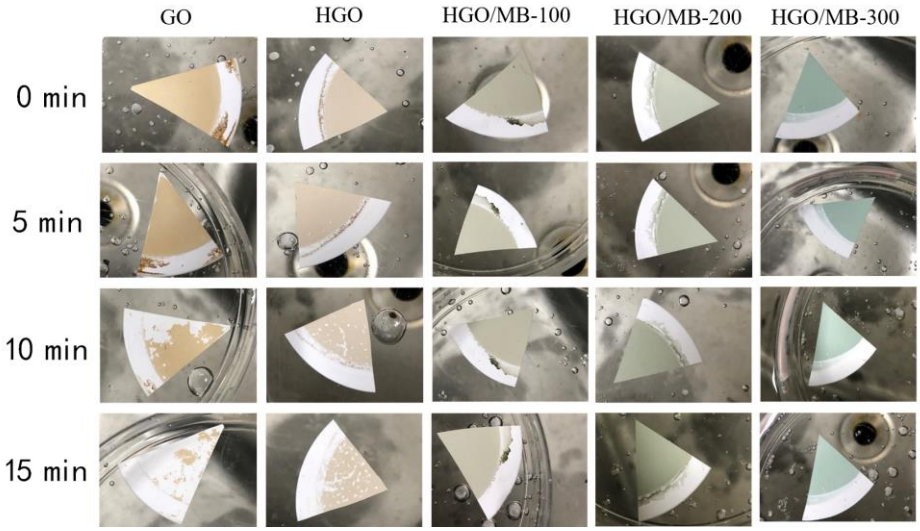

Figure 6. Stability of GO, HGO and HGO / MB membrane under ultrasound

4. Conclusions

We prepared HGO by chemical etching of GO with H_2O_2, and the nanopores on HGO provided additional transport channels to increase the water permeability. At the same time, MB was used to intercalate HGO. Membrane swelling in water was inhibited by π-π conjugation and electrostatic interactions between MB and HGO, so membrane stability and rejection performance were improved. Na_2SO_4 rejection rate of HGO/MB composite membrane reached 83.2% while the water flux (21.34 L/m_2·h·bar) was about 7 times higher than that of GO membrane. HGO/MB membrane showed rejection rates above 93% for both dyes, Rh B and MO, with the highest rejection rate of 95.9% for MO and 98.9% for Rh B. Thus, this study demonstrated that the HGO/MB membranes have effectively improved water flux and stability without loss of rejection, which held great potential for water treatment applications.

Acknowledgments

This project is supported by the National Natural Science Foundation of China (51005145, 510 75258) and the Key Laboratory for Thin Film and Microfabrication Technology of the Ministry of Education, Shanghai Jiaotong University.

References

1. Jiang, Y., Chai, L., Zhang, D., Ouyang, F., Zhou, X., Alhassan, S. I., Liu, S., He, Y., Yan, L., Wang, H., Zhang, W. (2022). Facet-controlled $LiMn_2O_4$/C as deionization electrode with enhanced stability and high desalination performance. Nano-Micro Letters, 14(1), Article 176. https://doi.org/10.1007/s40820-022-00897-3
2. Liu, X., Guo, Y., Zhang, C., Huang, X., Ma, K., Zhang, Y. (2022). Preparation of graphene oxide/4A molecular sieve composite and evaluation of adsorption performance for Rhodamine B. Separation and

Purification Technology, 286, Article 120400. https://doi.org/10.1016/j.seppur.2021.120400
3. Shen, S., Fu, J., Yi, J., Ma, L., Sheng, F., Li, C., Wang, T., Ning, C., Wang, H., Dong, K., Wang, Z. L. (2021). High-efficiency wastewater purification system based on coupled photoelectric-catalytic action provided by triboelectric nanogenerator. Nano-Micro Letters, 13(1), Article 194. https://doi.org/10.1007/s40820-021-00695-3
4. Wang, Z., Ma, C., Xu, C., Sinquefield, S.A., Shofner, M.L., Nair, S. (2021). Graphene oxide nanofiltration membranes for desalination under realistic conditions. Nature Sustainability, 4(5), 402-408. https://doi.org/10.1038/s41893-020-00674-3
5. Rashidi, H., Sulaiman, N.M.N., Hashim, N.A., Bradford, L., Asgharnejad, H., Larijani, M.M. (2020). Development of the ultra/nano filtration system for textile industry wastewater treatment. Membrane Water Treatment, 11(5), 333-344. https://doi.org/10.12989/mwt.2020.11.5.333
6. Meftah, N., Ezzeddine, A., Bedoui, A., Hannachi, A. (2020). Hybrid neutralization and membrane process for fluoride removal from an industrial effluent. Membrane Water Treatment, 11(4), 303-312. https://doi.org/10.12989/mwt.2020.11.4.303
7. Jung, J., Shin, B., Park, K.Y., Won, S., Cho, J. (2019). Pilot scale membrane separation of plating wastewater by nanofiltration and reverse osmosis. Membrane Water Treatment, 10(3), 239-244. https://doi.org/10.12989/mwt.2019.10.3.239
8. Wang, J., Zhu, J., Zhang, Y., Liu, J., Van der Bruggen, B. (2017). Nanoscale tailor-made membranes for precise and rapid molecular sieve separation. Nanoscale, 9(9), 2942-2957. https://doi.org/10.1039/c6nr08417f
9. Werber, J.R., Osuji, C.O., Elimelech, M. (2016). Materials for next-generation desalination and water purification membranes. Nature Reviews Materials, 1(4), 1-15. https://doi.org/10.1038/natrevmats.2016.18
10. Zhang, P., Gong, J.L., Zeng, G.M., Song, B., Cao, W., Liu, H.Y., Huan, S.Y., Peng, P. (2019). Novel "loose" GO/MoS_2 composites membranes with enhanced permeability for effective salts and dyes rejection at low pressure. Journal of Membrane Science, 574, 112-123. https://doi.org/10.1016/j.memsci.2018.12.046
11. Kumar, R., Verma, S., Harwani, G., Patidar, D., Mishra, S. (2022). Adsorptive and kinetic studies of toxic metal ions from contaminated water by functionalized silica. Membrane Water Treatment, 13(5), 227-233. https://doi.org/10.12989/mwt.2022.13.5.227
12. Huang, X., Li, L., Zhao, S., Tong, L., Li, Z., Peng, Z., Lin, R., Zhou, L., Peng, C., Xue, K.H., Chen, L., Cheng, G.J., Xiong, Z., Ye, L. (2022). MOF-like 3D graphene-based catalytic membrane fabricated by one-step laser scribing for robust water purification and green energy production. Nano-Micro Letters, 14(1), Article 174. https://doi.org/10.1007/s40820-022-00923-4
13. Zhou, S., Zhu, J., Wang, Z., Yang, Z., Yang, W., Yin, Z. (2022). Defective MOFs-based electrocatalytic self-cleaning membrane for wastewater reclamation: Enhanced antibiotics removal, membrane fouling control and mechanisms. Water Research, 220, Article 118635. https://doi.org/10.1016/j.watres.2022.118635
14. Bodzek, M., Konieczny, K., Kwiecińska-Mydlak, A. (2022). Recent advances in water and wastewater treatment using membranes with carbon nanotubes. Membrane Water Treatment, 13(6), 259-290. https://doi.org/10.12989/mwt.2022.13.6.259
15. Karahan, H.E., Goh, K., Zhang, C.J., Yang, E., Yıldırım, C., Chuah, C.Y., Ahunbay, M.G., Lee, J., Tantekin-Ersolmaz, S.B., Chen, Y., Bae, T.H. (2020). MXene materials for designing advanced separation membranes. Advanced Materials, 32(18), Article 1906697. https://doi.org/10.1002/adma.201906697
16. Lei, Z., Sun, X., Zhu, S., Dong, K., Liu, X., Wang, L., Zhang, X., Qu, L., Zhang, X. (2021). Nature-inspired MXene-decorated 3D honeycomb-fabric architectures toward efficient water desalination and salt harvesting. Nano-Micro Letters, 14(1), Article 10. https://doi.org/10.1007/s40820-021-00748-7
17. Dai, H., Liu, X., Zhang, C., Ma, K., Zhang, Y. (2021). Electrospinning polyacrylonitrile/graphene oxide/polyimide nanofibrous membranes for high-efficiency PM2.5 filtration. Separation and Purification Technology, 276, Article 119243. https://doi.org/10.1016/j.seppur.2021.119243

18. Liu, X., Guo, Y., Zhang, C., Huang, X., Ma, K., Zhang, Y. (2022). Preparation of graphene oxide/4A molecular sieve composite and evaluation of adsorption performance for Rhodamine B. Separation and Purification Technology, 286, Article 120400. https://doi.org/10.1016/j.seppur.2021.120400
19. Liu, Y., Bai, Z., Lin, G., Wang, L., Xu, X., He, L., Liu, X. (2022). Covalent cross-linking mediated TA-APTES NPs to construct a high-efficiency GO composite membrane for dye/salt separation. Applied Surface Science, 584, Article 152595. https://doi.org/10.1016/j.apsusc.2022.152595
20. Su, J., Jia, M., Wu, W., Li, Z., Li, W. (2020). Chemical vapor crosslinking of graphene oxide membranes for controlling nanochannels. Environmental Science: Nano, 7(10), 2924-2929. https://doi.org/10.1039/D0EN00710B
21. Sabna, V., Thampi, S.G., Chandrakaran, S., Sasina, E.P., Resmi, P. (2021). fMWNTs/GO/MnO 2 nanocomposites as additives in a membrane for the removal of crystal violet. Membrane and Water Treatment, 12(5), 205-216. https://doi.org/10.12989/mwt.2021.12.5.205
22. Zahoor, A., Naqvi, A.A., Butt, F.A., Zaidi, G.R., Younus, M. (2022). Effect of graphene oxide on polyvinyl alcohol membrane for textile wastewater treatment. Membrane Water Treatment, 13(3), 121-128. https://doi.org/10.12989/mwt.2022.13.3.121
23. Azamat, J. (2021). Application of graphene, graphene oxide, and boron nitride nanosheets in the water treatment. Membrane Water Treatment, 12(5), 227-243. https://doi.org/10.12989/mwt.2021.12.5.227
24. Fan, X., Cai, C., Gao, J., Han, X., Li, J. (2020). Hydrothermal reduced graphene oxide membranes for dyes removing. Separation and Purification Technology, 241, Article 116730. https://doi.org/10.1016/j.seppur.2020.116730
25. Pandey, R.P., Kallem, P., Hegab, H.M., Rasheed, P.A., Banat, F., Hasan, S.W. (2022). Cross-linked laminar graphene oxide membranes for wastewater treatment and desalination: A review. Journal of Environmental Management, 317, Article 115367. https://doi.org/10.1016/j.jenvman.2022.115367
26. Wang, S., Liang, S., Chen, L., Fang, H. (2022). Realizing ultrahigh nanofiltration performance based on small flake reduced graphene oxide membranes. Desalination, 528, Article 115601. https://doi.org/10.1016/j.desal.2022.115601
27. Zheng, S., Tu, Q., Urban, J.J., Li, S., Mi, B. (2017). Swelling of graphene oxide membranes in aqueous solution: Characterization of interlayer spacing and insight into water transport mechanisms. ACS Nano, 11(7), 6440-6450. https://doi.org/10.1021/acsnano.7b02999
28. Li, Y., Yuan, S., Xia, Y., Zhao, W., Easton, C. D., Selomulya, C., Zhang, X. (2020). Mild annealing reduced graphene oxide membrane for nanofiltration. Journal of Membrane Science, 601, Article 117900. https://doi.org/10.1016/j.memsci.2020.117900
29. Hou, J., Chen, Y., Shi, W., Bao, C., Hu, X. (2020). Graphene oxide/methylene blue composite membrane for dyes separation: Formation mechanism and separation performance. Applied Surface Science, 505, Article 144145. https://doi.org/10.1016/j.apsusc.2019.144145
30. Shen, H., Wang, N., Ma, K., Wang, L., Chen, G., Ji, S. (2017). Tuning inter-layer spacing of graphene oxide laminates with solvent green to enhance its nanofiltration performance. Journal of Membrane Science, 527, 43-50. https://doi.org/10.1016/j.memsci.2017.01.003
31. Hou, R., He, Y., Yu, H., Ma, J., Gao, Y., Bai, Y., Chen, J. (2021). Intercalation of N-doped graphene into graphene oxide-based membranes to improve their overall nanofiltration performance. Chemical Physics Letters, 775, Article 138657. https://doi.org/10.1016/j.cplett.2021.138657
32. Chen, X., Feng, Z., Gohil, J., Stafford, C.M., Dai, N., Huang, L., Lin, H. (2020). Reduced holey graphene oxide membranes for desalination with improved water permeance. ACS Applied Materials & Interfaces, 12(1), 1387-1394. https://doi.org/10.1021/acsami.9b19255
33. Ding, A., Ren, Z., Zhang, Y., Ma, J., Bai, L., Wang, B., Cheng, X. (2021). Evaluations of holey graphene oxide modified ultrafiltration membrane and the performance for water purification. Chemosphere, 285, Article 131459. https://doi.org/10.1016/j.chemosphere.2021.131459
34. Buelke, C., Alshami, A., Casler, J., Lin, Y., Hickner, M., Aljundi, I. H. (2019). Evaluating graphene oxide and holey graphene oxide membrane performance for water purification. Journal of Membrane Science, 588, Article 117195. https://doi.org/10.1016/j.memsci.2019.117195
35. Li, Y., Zhao, W., Weyland, M., Yuan, S., Xia, Y., Liu, H., Jian, M., Yang, J., Easton, C.D., Selomulya,

C., Zhang, X. (2019). Thermally reduced nanoporous graphene oxide membrane for desalination. Environmental Science & Technology, 53(14), 8314-8323. https://doi.org/10.1021/acs.est.9b01914

36. Huang, L., Huang, S., Venna, S.R., Lin, H. (2018). Rightsizing nanochannels in reduced graphene oxide membranes by solvating for dye desalination. Environmental Science & Technology, 52(21), 12649-12655. https://doi.org/10.1021/acs.est.8b03661
37. Ma, H., Wang, G., Xu, Z., Dong, X., Zhang, X. (2022). Confining peroxymonosulfate activation in carbon nanotube intercalated nitrogen doped reduced graphene oxide membrane for enhanced water treatment: The role of nanoconfinement effect. Journal of Colloid and Interface Science, 608, 2740-2751. https://doi.org/10.1016/j.jcis.2021.11.007
38. Hu, Z., Cui, H., Zhu, Y., Lei, G., Li, Z. (2022). Holey reduced graphene oxide nanosheets wrapped hollow FeS2@C spheres as a high-performance anode material for sodium-ion batteries. Journal of Power Sources, 536, Article 231438. https://doi.org/10.1016/j.jpowsour.2022.231438
39. Xu, Y., Chen, C.Y., Zhao, Z., Lin, Z., Lee, C., Xu, X., Wang, C., Huang, Y., Shakir, M.I., Duan, X. (2015). Solution processable holey graphene oxide and its derived macrostructures for high-performance supercapacitors. Nano Letters, 15(7), 4605-4610. https://doi.org/10.1021/acs.nanolett.5b01212
40. Kang, K.M., Kim, D.W., Ren, C.E., Cho, K.M., Kim, S.J., Choi, J.H., Nam, Y.T., Gogotsi, Y., Jung, H.T. (2017). Selective molecular separation on Ti_3C_2Tx-graphene oxide membranes during pressure-driven filtration: Comparison with graphene oxide and MXenes. ACS Applied Materials & Interfaces, 9(51), 44687-44694. https://doi.org/10.1021/acsami.7b10932
41. Akbari, A., Sheath, P., Martin, S.T., Shinde, D.B., Shaibani, M., Banerjee, P.C., Tkacz, R., Bhattacharyya, D., Majumder, M. (2016). Large-area graphene-based nanofiltration membranes by shear alignment of discotic nematic liquid crystals of graphene oxide. Nature Communications, 7, Article 10891. https://doi.org/10.1038/ncomms10891
42. Montes-Navajas, P., Asenjo, N.G., Santamaría, R., Menéndez, R., Corma, A., García, H. (2013). Surface area measurement of graphene oxide in aqueous solutions. Langmuir, 29(44), 13443-13448. https://doi.org/10.1021/la4029904
43. Xu, X.L., Lin, F.W., Du, Y., Zhang, X., Wu, J., Xu, Z.K. (2016). Graphene oxide nanofiltration membranes stabilized by cationic porphyrin for high salt rejection. ACS Applied Materials & Interfaces, 8(19), 12588-12593. https://doi.org/10.1021/acsami.6b03693
44. Lee, K.H., Kang, D.J., Eom, W., Lee, H., Han, T.H. (2022). Holey graphene oxide membranes containing both nanopores and nanochannels for highly efficient harvesting of water evaporation energy. Chemical Engineering Journal, 430, Article 132759. https://doi.org/10.1016/j.cej.2021.132759